24th COBEM - 2017

24th ABCM International Congress of Mechanical Engineering
December 3-8, 2017, Curitiba, PR, Brazil

COBEM2017-1909
EXPERIMENTAL ANALYSIS OF NUCLEATE BOILING ON NANOSTRUCTURED SURFACES UNDER CONFINED CONDITIONS

Jéssica Martha Nunes
UNESP - Univ Estadual Paulista, Department of Mechanical Engineering, Av. Brasil Centro, 56, 15385-000 Ilha Solteira, SP, Brazil
je.nunes25@gmail.com

Leonardo Lachi Manetti
UNESP - Univ Estadual Paulista, Department of Mechanical Engineering, Av. Brasil Centro, 56, 15385-000 Ilha Solteira, SP, Brazil
leomanetti@gmail.com

Elaine Maria Cardoso
UNESP - Univ Estadual Paulista, Department of Mechanical Engineering, Av. Brasil Centro, 56, 15385-000 Ilha Solteira, SP, Brazil
elainemaria@dem.feis.unesp.br

Abstract. *Nanocoating techniques have been used to increase the heat transfer coefficient by changing the surface morphology, which could potentially increase the heat transfer in case of pool boiling systems. The present work aims to study the effect of nanostructured surfaces and the gap size during the nucleate boiling of DI-water, at atmospheric pressure and saturation temperature. The tests were performed on copper heating rough surfaces. The nanostructured surfaces were produced by maghemite nanoparticle deposition, for two different mass concentrations, via nanofluid boiling process. A gap size of 1.0 mm (Bo = 0.4) and of 13 mm (corresponding to an unconfined case, Bo = 5.2) were analyzed in this study. Concerning the heat transfer coefficient for the unconfined case, it was observed that both nanostructured rough surfaces showed deterioration of HTC when compared with the surface without deposition due to the fouling resistance formed on the heating surface. For the confined case, the enhanced boiling is a consequence of the deformed bubbles which increase the area of the liquid film between the vapor bubble and the heating surface, which increased the HTC up to 22%.*

Keywords: *Boiling heat transfer, nanostructured surface, confined nucleate boiling.*

1. INTRODUCTION

The technology advance of electronic devices with high processing capacity and reduced size pointed out the need to study more efficient heat transfer methods. In this way, new techniques to improve the heat transfer have been researched. One of them is the heat transfer due to phase change, in other words, boiling processes, which is widely diffused by the scientific community due to its high heat removal capacity. Moreover, in the last ten years, the application of nanotechnology in the heat transfer by using nanoparticles, nanofluids, and nanostructures for improving the heat transfer on electronic devices also has been studied.

The first study on the effect of surface characteristics on the boiling process was done by Fritz (1935) and since then, methods of surface modification have been proposed in order to increase the heat transfer coefficient (HTC) and the critical heat flux (CHF). Among studies related to nanofluids, Das et al. (2003) and Bang and Chang (2005) reported the effect of surface modification through nanofluid boiling - called nanostructures. As reported by Manetti and Cardoso (2015), both the HTC and the CHF behaviors may be attributed to changes in the surface wettability and morphology caused by the nanoparticle deposition.

Manetti et al. (2017) used alumina-water based nanofluid in pool boiling and verified that the nanoparticle deposition rate increases as the heat flux increases; moreover, the nanoparticle deposition is a function of boiling time and nanofluid concentration. According to the authors, the cavity radius seems to play a more important role on the heat transfer behavior, as for moderated heat flux and for low nanofluid concentration, larger cavity radii require less wall superheating to be activated, that results in higher HTC values. HTC degradation with increasing heat flux was observed for high nanofluid concentration, regardless of the surface roughness, due to the increase of the thermal resistance of the heating surface.

Kiyomura et al. (2017) carried out studies on maghemite nanostructured surfaces deposited through the boiling process of maghemite-water based nanofluid. The nanocoating modified the roughness and wettability of the heating surface, leading to an increase or decrease of HTC. For the case of HTC enhancement, the authors reported that the nanocoating increases the surface roughness, leading to an increase in the nucleation site density. Also, the static contact angle decreases compared to the original surface (surface without deposition). However, in the case of HTC degradation, the thermal resistance due to the nanoparticle deposition overlaps the effect of the surface roughness improvement, implying the HTC deterioration.

The use of boiling for cooling microelectronic components implies the study of this phenomenon in confined systems, where the distance between the surface to be cooled and an adiabatic surface is smaller than the diameter of the vapor bubbles, changing the mechanisms responsible for the thermal performance. When the gap size (s) where the boiling occurs is lower than the bubble diameter, the thermal and hydrodynamic characteristics of the heat transfer are different from those observed in free boiling (Cardoso and Passos, 2013). Under confined conditions, the vapor bubbles are deformed and stay longer in the confined space. Figures 1a and 1b show the vapor bubble behavior under unconfined and confined conditions, respectively.

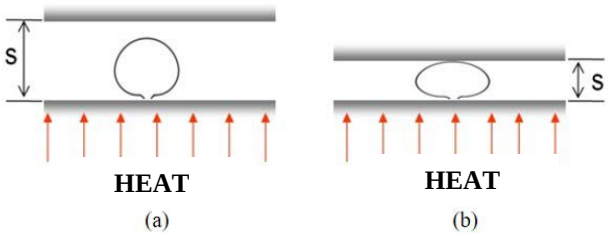

Figure 1. Vapor bubble growth: (a) unconfined case; (b) confined case.

The gap size effect can be characterized by a dimensionless number known as the Bond number, *Bo*, defined as the ratio of the characteristic length to the confined space, *s*, and the capillary length, L_b (proportional to the detachment diameter of the vapor bubble). Thus, the HTC can also be modified by the confinement of the system using, for example, an unheated surface, where if the vapor bubble diameter is less than the characteristic length, *s*, the Bond number is higher than 1 ($Bo > 1$). However, if the capillary length is higher than *s*, $Bo < 1$, the bubbles will deform and coalescence with the neighboring bubbles, increasing the microlayer contact area between the heating surface and the vapor bubble and thus intensifying the heat transfer according to Katto et al. (1977) and Ishibashi and Nishikawa (1969).

Stutz et al. (2009) studied the behavior of the CHF as a function of confinement in the saturated boiling regime by using n-Pentane as working fluid and copper facing upward as heated surface. They showed that when the distance *s* reaches a value close to the capillary length L_b, significant changes in the phenomenon of heat transfer occur. Katto et al. (1977) showed similar trends in their study by using water as working fluid. Such researchers have shown that reducing the gap size or increasing the level of confinement leads to the accumulation of vapor bubbles between the surfaces for high heat flux values. The confinement increases the waiting time of the vapor bubble, causing an earlier occurrence of the CHF as compared to the same heated surface without confinement.

Souza et al. (2014) studied the effect of maghemite nanoparticle deposition on a heated copper surface during the nucleate boiling of HFE7100, at saturation temperature and at atmospheric pressure. Two different nanoparticle diameters (10 nm and 80 nm) were investigated, and also, it was considered two experimental conditions: confined and unconfined boiling. The results showed an enhancement of around 55% in the HTC for the nanostructured surface with the smallest nanoparticle diameter compared to the surface without deposition. For the largest nanoparticle diameter, the results showed a decrease of 29% in the HTC compared to the case without nanoparticle deposition.

In this context, the present work aims to analyze the nucleate boiling of DI-water using nanostructured surfaces under confined and unconfined conditions. The use of DI-water as working fluid allows us to verify the influence of nanostructured surfaces and gap size on the surface/fluid interaction (such as surface roughness and wettability), and consequently, on the HTC and CHF.

2. MATERIALS AND METHODS

2.1 Test surfaces preparation

Table 1 shows the conditions tested in this study. The surfaces analyzed consisted of one rough surface without deposition (RS) and two rough surfaces with nanoparticle deposition (RS-LC and RS-HC). In order to coat the copper heating surface, the maghemite nanofluid (Fe_2O_3-deionized water) was boiled at two different concentrations - 0.03 g/l (low concentration, LC) and 0.3 g/l (high concentration, HC).

All the surfaces were polished with #400 emery paper, which corresponds an average roughness (R_a) of 0.44 μm. After the polishing process, in order to clean the surfaces, they were put into an ultrasonic bath during 5 minutes and cleaned with acetone.

The maghemite (γ –Fe_2O_3 with average particle size of 10 nm) nanoparticles were synthesized following Massart's method (Massart, 1982) through the precipitation of Fe^{2+} and Fe^{3+} salts in alkaline medium and dispersed in water. The Fe_2O_3-deionized water nanofluid was supplied by Prof. Maria de Fátima da Silva from NFA/ Instituto de Física/ Universidade de Brasília.

Table 1. Description of the experimental conditions tested in the present study.

Heating Surface	Nanofluid concentration	Gap size, *s* (mm)
Rough Surface, RS (manually polished with #400 emery paper)	Without deposition	1.0 (RS-Confined) 13.0 (RS-Unconfined)
	0.03 g/l (LC)	1.0 (RS-LC-Confined) 13.0 (RS-LC-Unconfined)
	0.3 g/l (HC)	1.0 (RS-HC-Confined) 13.0 (RS-HC-Unconfined)

For each surface configuration, two levels of confinement are tested, which is given by the dimensionless Bond number (*Bo*), where $Bo < 1$ represents confined surfaces (s = 1.0 mm, Bo = 0.4) and $Bo > 1$ (s = 13.0 mm, Bo = 5.2) represents unconfined surfaces. The spacing between the heating surface and the adiabatic upper surface is represented by the variable *s*. In order to validate the boiling setup, pure DI-water tests were carried out on the rough surface, namely RS.

2.2 Apparatus assembly

The experimental setup, Fig. 2, is composed by a test section, two thermostatic baths, an electrical power source, a data acquisition Agilent 34970A model, and a computer.

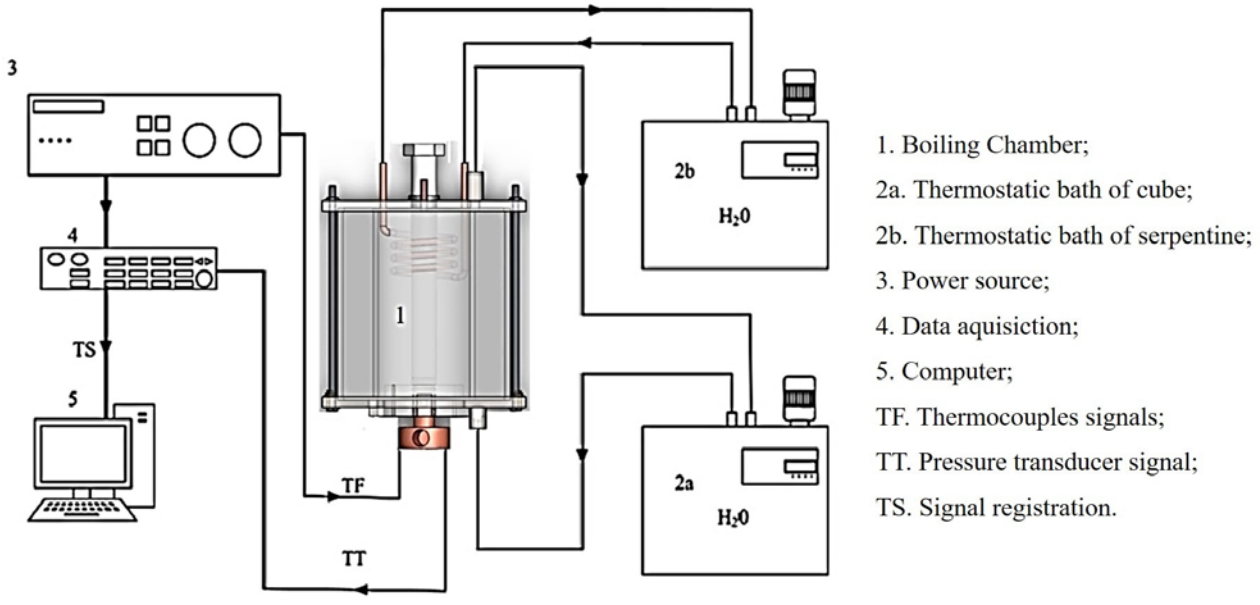

Figure 2. Schematic drawing of the experimental apparatus.

The boiling chamber (Fig. 3) consists of a cube vessel of 5 mm thick glass walls and overall dimensions 170 x 170 x 180 mm, which involves a borosilicate tube of 90 mm internal diameter, 180 mm height, and 6 mm wall thickness. The cube vessel and the tube are fixed between two plates of stainless steel (AISI 316). Inside the tube, there is a condenser made by a copper serpentine and the element for confinement (Fig. 3). The element for confinement has 250 mm in length and 20 mm in diameter.

In the space between the vessel and the glass tube, there is a forced flow of water whose temperature is controlled by a thermostatic bath, in order to maintain the temperature of the working fluid near the saturation temperature (at

atmospheric pressure, T_{sat} = 99 °C). A second thermostatic bath is used to control the temperature of the condenser located at the top of the boiling chamber.

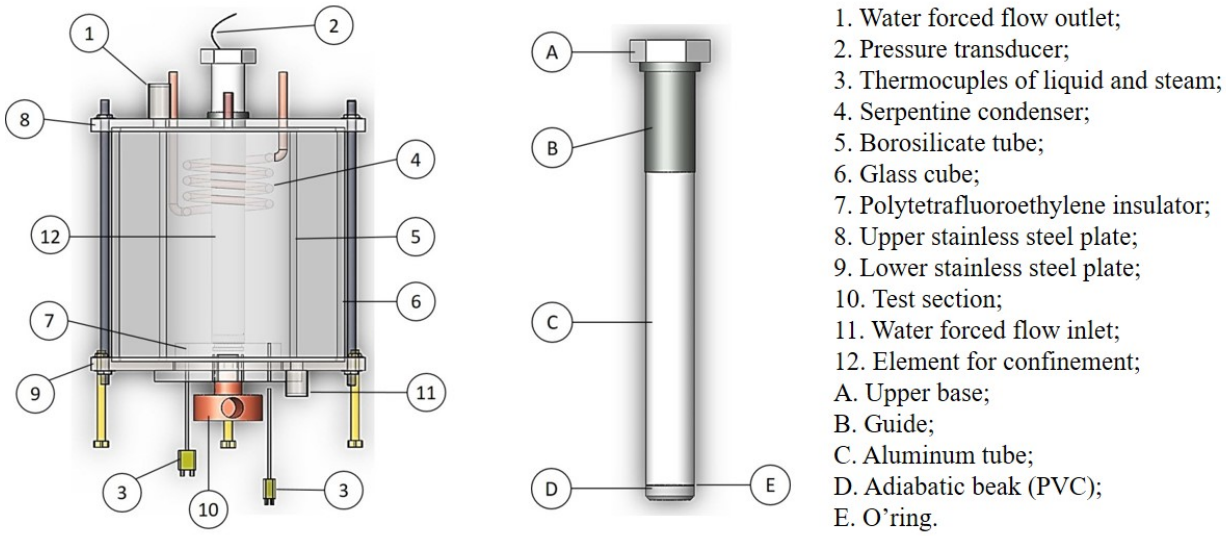

Figure 3. Boiling chamber and details of the element for confinement.

The test section consists of a copper block (20 mm diameter) with three K-type thermocouples, with hot junctions diameters of 0.50 mm fixed inside 1 mm diameter holes at the radial center of the copper cylinder, fixed in the cylindrical part (Fig. 4), to determine the wall temperatures and the heat flux. The copper block is heated by one cartridge resistance with a maximum power of 300 W. The thermal insulation of the test section consists of polytetrafluoroethylene and vermiculite.

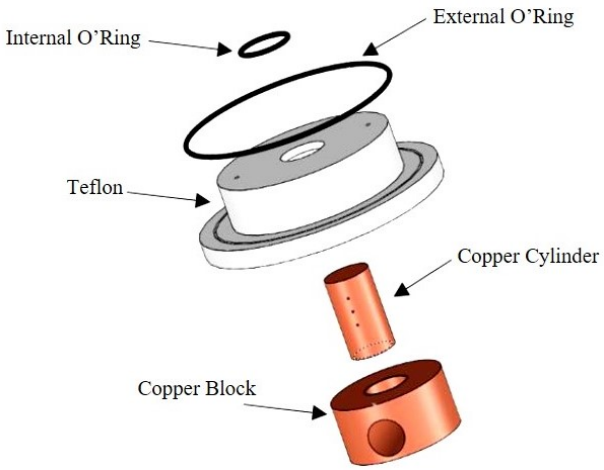

Figure 4. Test section – exploded view.

2.3 Experimental Procedure

The experiments were conducted using deionized water as the working fluid under saturated conditions at a pressure close to 98 kPa. Before each run, the working fluid was heated very close to the saturation temperature in order to degas it. No evidence of significant amounts of gas dissolved in the working fluid was detected on the boiling curves. Before each series of measurements, vacuum was created in the boiling chamber and, then, this vessel was immediately fed with the working fluid. The test conditions were regulated by monitoring the pressure and the temperature inside the boiling chamber. The same procedure was adopted during all the experimental tests in order to ensure repeatability.

When the apparatus reaches the saturation temperature in a steady state, heat fluxes in a range of 100 to 800 kW/m² were applied increasing in steps of 100 kW/m² - for unconfined cases – and 60 kW/m² - for the confined cases. The CHF was characterized by the non-stability of heating surface temperature.

The heat flux and surface temperature are calculated according to Fourier's Law assuming 1-D conduction based on the wall temperature measurements from the thermocouples embedded in the copper block. The temperature of the boiling surface was then determined by extrapolating the linear temperature profile to the copper block upper surface, T_w. The setup of the block and the location of the thermocouples are shown in Fig. 5.

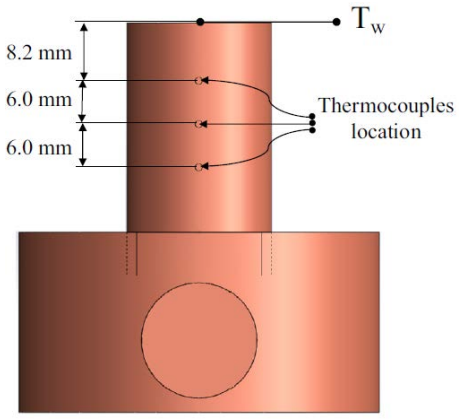

Figure 5. Copper heating surface.

Moreover, a comparison between the imposed heat flux based on the current and voltage measurements, and the heat flux estimated from the linear profile reveals heat losses always lower than 15%.

Finally, the heat transfer coefficient was calculated using Newton's law of cooling given by:

$$h = \frac{q''}{\Delta T_{sat}} \tag{1}$$

where $\Delta T_{sat} = T_w - T_{sat}(p_{atm})$. T_w is the wall temperature, and $T_{sat}(p_{atm})$ corresponds to the saturation temperature of water at local atmospheric pressure (p_{atm} = 98 kPa).

The temperature uncertainty was ± 0.4 ºC. For all surfaces tested, the experimental uncertainty for the heat flux and for the HTC varied from 1.6% to 15.3%, and from 2.6% to 15.9%, respectively.

2.4 Wettability measurement

Figure 6 presents the experimental apparatus used to capture images of the sessile drops before being analyzed for static and dynamic contact angles. It consists of a test surface, a camera, a green LED light source, a light diffuser and an aluminum plate where the test surface is fixed. In this apparatus, it is possible to measure the advancing and receding contact angles by altering its inclination through a stepper motor connected to an Arduino board.

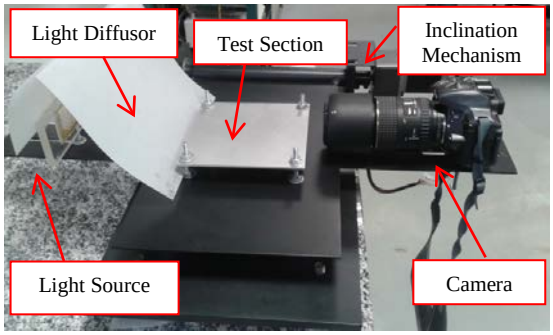

Figure 6. Experimental setup used to capture the sessile drops images.

The procedure adopted to evaluate the contact angle consists on depositing on the test surface a sessile droplet of water with a volume of 20 µl through a syringe pointed vertically down onto the sample. Then, images of the droplet on the surface are captured by a camera. After that, the pictures are analyzed using image post-processing software to shape the deionized water droplet. The adopted procedure is well detailed by Da Cunha et al. (2017).

3. RESULTS AND DISCUSSION

Table 2 presents the roughness, R_a (μm), and the static contact angles for all surfaces tested in this work. The results showed that the surface roughness and the static contact angle depend on the nanofluid concentration. As nanofluid concentration increases the surface roughness, wettability and nanolayer thickness also increase. All these parameters strongly affect the dynamic of vapor bubble growth and detachment, and consequently, the heat transfer.

The images in Tab. 2 depicts surface-fluid interaction conditions of the sessile droplets onto the rough surfaces before and after nanofluid pool boiling process using pure water droplet. According to the results displayed, the heating surface wettability and the static contact angle are a function of the nanofluid concentration and the original surface condition. As the nanofluid concentration increases, the contact angle decreases and consequently enhances the surface wettability. These results agree with Takata et al. (2005) who reported that surface wettability is inversely proportional to contact angle.

Table 2. Average surface roughness and static contact angle.

Surfaces	R_a **(μm)**	**Superficial interaction with DI – Water Droplets (Contact angle)**
Rough surface without deposition (RS)	0.44	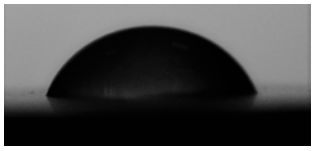 70°
Rough nanocoated surface at low concentration (RS-LC)	0.56	 20°
Rough nanocoated surface at high concentration (RS-HC)	1.01	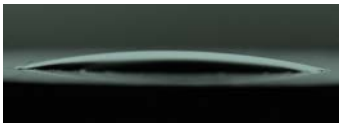 <10°

The Fig. 7 compares the confined (s = 1.0 mm, $Bo < 1$) and unconfined (s = 13.0 mm, $Bo > 1$) tests. One may observe that the confinement promoted an intensification of the boiling heat transfer for all the cases, mainly for low and moderated heat fluxes, as compared to the case without confinement. The bubble deformation and the increase in the residence time of the vapor bubbles on the heating surface promote the liquid film evaporation present between the heating surface and the vapor bubble, leading to an increase in the HTC. For the rough surface without deposition (RS), the HTC increased 22% for heat fluxes up to 350 kW/m² (low heat fluxes) due to the confinement effect. In the case of nanostructured surfaces, for nanostructures at low concentration (RS-LC) the HTC increased 15%, and for nanostructured surfaces at high nanofluid concentration (RS-HC), the HTC increased 9%, being all of them analyzed for low heat fluxes (up to 350 kW / m²).

Increasing the heat flux the bubble frequency also increases, creating a large mass of vapor in the channel that inhibits the cooling effect of the heating surface; thus, it anticipates the dryout phenomenon and degrades the HTC.

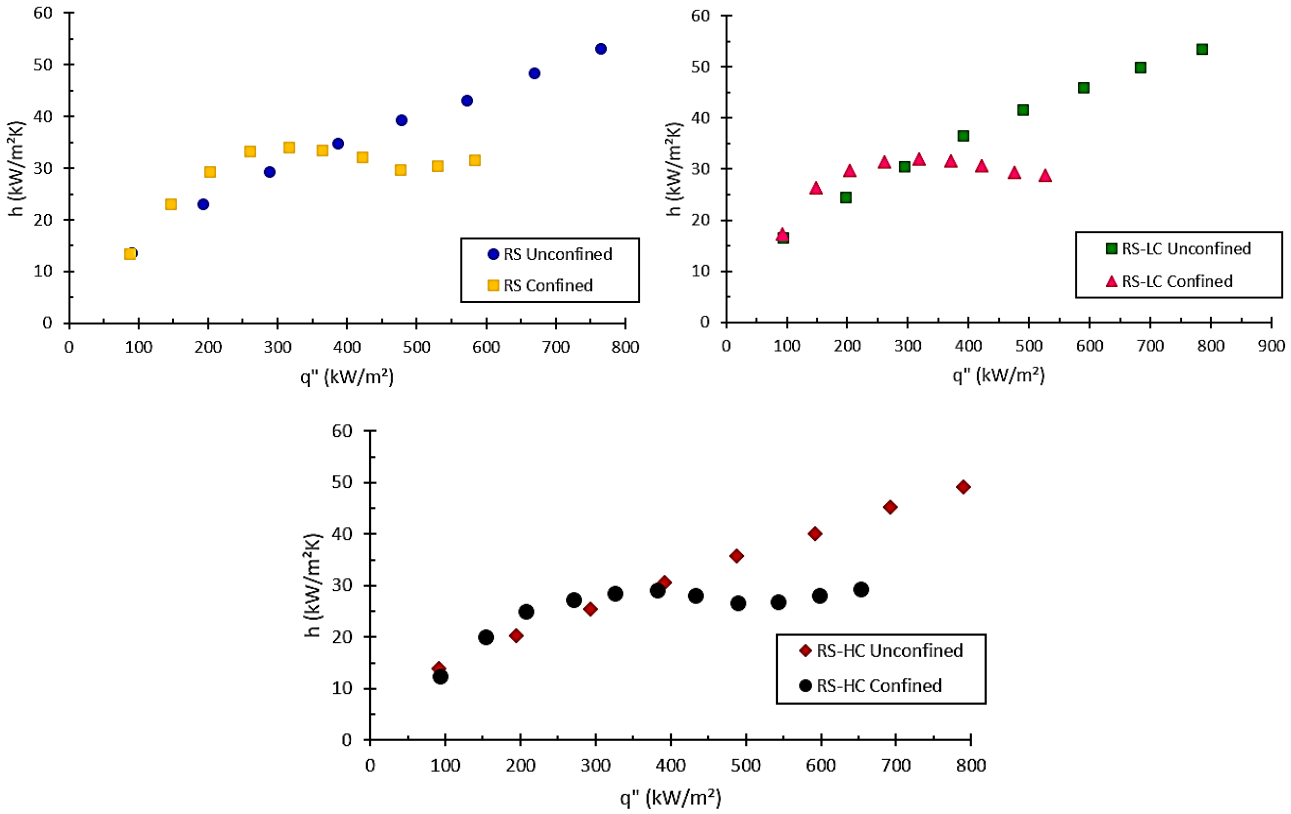

Figure 7. HTC curves for rough surfaces under confined and unconfined cases.

Figure 8 shows the images taken during the test with RS, at low heat flux (100 kW/m²) and at medium heat fluxes (640 kW/m², corresponding to the heat flux close to the CHF). One may observe that, for low heat flux value (Fig. 8a) the bubbles are small and there is no vapor entrapped between the surface and the confinement element. Instead, for moderated heat flux value (Fig. 8b), it is noticeable the coalescence of the vapor bubbles that get trapped between the surface and the confinement element.

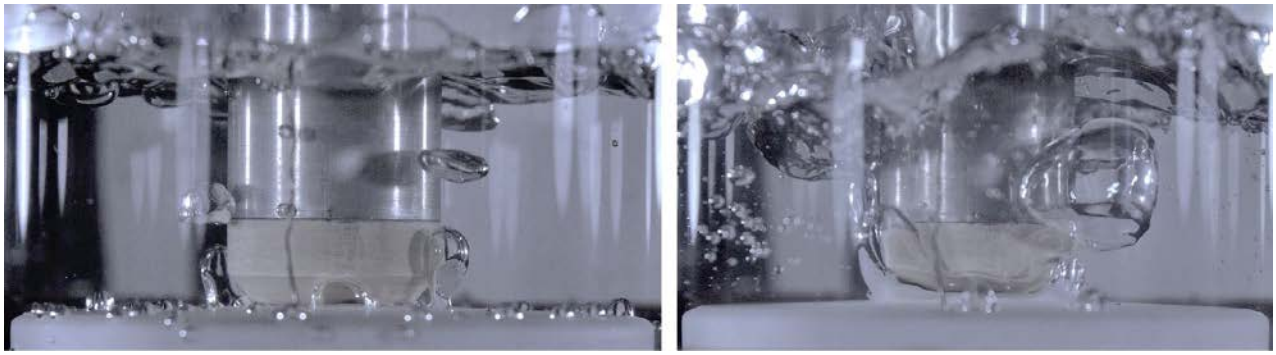

Figure 8. RS test images for low and moderated heat flux applied. a) for 100 kW/m² and b) for 640 kW/m², respectively.

The Fig. 9 shows the HTC curves for the unconfined case ($Bo > 1$) and confined case ($Bo < 1$) for rough surfaces. For the unconfined tests, both of RS-HC-Unconfined and RS-LC-Unconfined surfaces showed a HTC degradation as compared to the heating surfaces without deposition, RS-Unconfined. This occurs because the decrease in the bubble frequency and its departure diameter, since the cavities are filled with the nanoparticles. As the nanofluid concentration increases the nanolayer formed on the heating surface also increases, leading to an enhancement in the thermal resistance and HTC degradation. The similar behavior can be observed in the curves for the confined tests ($Bo < 1$), where the nanocoated surface did not promote an increment in HTC average value compared to the case of confined surface without deposition. However, the nanocoating leads to a dryout delay in the confined tests, which can be explained by the fact that the nanostructures influence the surface/fluid interaction mechanisms, increasing the wettability of the surface, which is a pronounced effect for non-wetting fluids, as the DI-water.

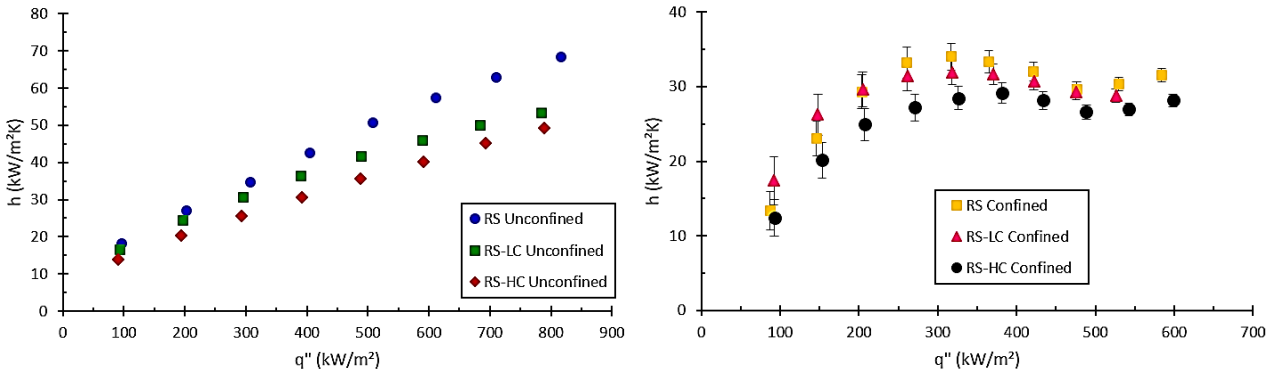

Figure 9. HTC curves for rough surfaces with and without nanoparticle deposition – unconfined and confined cases.

As the surface wettability increase, the re-wetting during the boiling process also increases, increasing the surface cooling. For confined conditions, the vapor mass trapped in the channel inhibits the re-wetting process and, the RS reaches the dryout earlier as compared to the nanostructured surfaces. For confined case, through polynomial adjustment, it was possible to determine the dryout heat flux by the maximum points of the HTC curves. For the RS-LC, the dryout occurred at 390 kW/m², increasing 8% compared with the RS; and, for the RS-HC, the dryout occurred at 400 kW/m², increasing 11% compared with the RS.

4. CONCLUSION

An analysis on the effect of surface roughness and nanofluid concentration on the HTC, using DI-water as working fluid, in confined and unconfined conditions, were carried out. A roughness and wettability characterization, after the deposition process by nanofluid pool boiling technique, were presented. The main results are summarized as follows:

- ✓ Increasing the nanofluid concentration used for nanocoating, it increases the surface average roughness. The nanostructure causes an increase in the surface wettability, which is characterized by the decrease in the static contact angle.
- ✓ The coated layer formed on the rough surfaces provides a barrier to the heat transfer and reduces the vapor bubble nucleation, which may lead to a reduction in the number of microcavities and an increase in the thermal resistance of the surface, therefore degrading the HTC, for both confined and unconfined cases;
- ✓ The confinement causes an increase in the HTC, due to the fact that the vapor bubbles coalesce and stay longer on the heating surface, promoting the evaporation of the liquid film presented between the heated surface and the vapor bubble. This effect, however, only occurs for low heat fluxes applied. The increase in the heat flux leads to the formation of a mass of vapor trapped on the heated surface, anticipating the dryout phenomenon and, consequently, reaching the CHF earlier than for unconfined cases;
- ✓ The nanostructure on rough surfaces does not increase the HTC; moreover, the deposition of the nanoparticles causes a clogging effect of the pre-existing cavity on the surface, degrading HTC for both confined and unconfined cases. However, for confined cases, the enhanced in the wettability caused by nanostructures helps to delay the dryout phenomenon.

5. ACKNOWLEDGEMENTS

The authors are grateful for the financial support from the PPGEM – UNESP/FEIS, from CAPES, from CNPq (grant number 458702/2014-5) and from FAPESP (grants numbers 2013/15431-7, 2014/19497-5 e 2016/02034-8). The authors also extend their gratitude to Mrs. Maria de Fátima da Silva and Mr. Marcelo Parise from NFA/Instituto de Física - UNB for supplying the nanofluids.

6. REFERENCES

Bang, I.C. and Chang, S.H., 2003. “Boiling heat transfer performance and phenomena of Al2O3 – water nanofluids from a plain surface in a pool”. *International Journal of Heat and Mass Transfer*, vol. 48, p. 2407.

Cardoso, E.M. and Passos, J.C., 2013. “Nucleate Boiling of *n*-Pentane in a Horizontal Confined Space”. *Heat Transfer Engineering*. Vol. 34, p. 470-478. DOI: 10.1080/01457632.2012.722438.

Da Cunha, A.P.; Mogaji, T.S. and Cardoso, E.M., 2017. "A Method for Measuring Contact Angle and for Analysing the Surface Wettability". In *9th World Conference on Experimental Heat Transfer, Fluid Mechanics and Thermodynamics – ExHFT2017*. Iguazu Falls, Brazil.

Das, S.K.; Putra, N. and Roetzel, W., 2003. "Pool boiling of nanofluids on horizontal narrow tubes". *International Journal of Multiphase Flow*, Vol. 29, p. 1237.

Fritz, W., 1935. "Maximum volume of vapor bubbles". *Phys. Z*, Vol. 36, p. 379.

Ishibashi, E. and Nishikawa, K., 1969. "Saturated boiling heat transfer in narrow spaces". *International Journal of Heat and Mass Transfer*, vol. 12, p. 863-893.

Katto, Y.; Yokoya, S. and Teraoka, K., 1977. "Nucleate and Transition Boiling in a Narrow Space Between Two Horizontal, Parallel Disk-Surfaces". *Bulletin of the JSME*, vol. 20, n°143, p. 638-643.

Kiyomura, I.S.; Manetti, L.L.; Da Cunha, A.P.; Ribatski, G. and Cardoso, E.M., 2017. "An analysis of the effects of nanoparticles deposition on characteristics of the heating surface and on pool boiling of water". *International Journal of Heat and Mass Transfer*, vol. 106, p. 666.

Manetti, L.L. and Cardoso, E.M., 2015. "Review of the Influence of Nanofluids on the Nucleate Pool Boiling". In *Proceedings of the 23rd International Congress of Mechanical Engineering - COBEM2015*. Rio de Janeiro, Brazil.

Manetti, L.L.; Mogaji, T.S.; Beck, P.A. and Cardoso, E.M., 2017. "Evaluation of the heat transfer enhancement during pool boiling using low concentrations of Al_2O_3-water based nanofluid". *Experimental Thermal and Fluid Science*, vol. 87, p. 191-200.

Massart, R., 1982. "Magnetic fluids and process for obtain them". *US Patent* 4329241.

Souza, R.R.; Passos, J.C. and Cardoso, E.M., 2014. "Influence of nanoparticle size and gap size on nucleate boiling using HFE7100", *Experimental Thermal and Fluid Science*, Vol. 59, pp. 195-201.

Stutz, B.; Lallemand, M.; Raimbault, F. and Passos, J.C., 2009. "Nucleate and transition boiling in narrow horizontal spaces". *Heat Mass Transfer*, vol. 45, p. 929–935.

Takata, Y., Hidaka, S., Cao, J.M., Nakamura, T., Yamamoto, H., Masuda, M. and Ito, T., 2005. "Effect of surface wettability on boiling and evaporation." *Energy* Vol. 30, pp. 209-220.

7. RESPONSIBILITY NOTICE

The authors are the only responsible for the printed material included in this paper.